MATHEMATICS AND COMPUTATIONAL SCIENCES

Vol 5(4), 2024, pp:26-47

DOI:10.30511/mcs.2024.2032110.1183

ISSN:2717-2708

http://mcs.qut.ac.ir/

Qom University of Technology

Investigating the effects of some controls measures on the dynamics of diphtheria infection using fractional order model

Loyinmi Adedapo Chris [1], Ijaola Alani Lateef [2]

Abstract: In this study, we presented a computationally intensive alternative and a suitable time-fractional order model to further comprehend the transmission dynamics of Diphtheria and study the overall effects of some control measures on its transmission. Public awareness (U_1), immediate treatment after being diagnosed (U_2) and the combination of both controls (U_3) are the three measures considered and all parameters and conditions that guarantee feasible of the proposed SEIR model: uniqueness and existence of solutions, the reproduction number, boundedness and positivity of solutions, global and local stability analysis of the disease-free equilibrium state was thoroughly analyzed and established, the Adam's Bashforth predictor-corrector method was utilized for the numerical solution, More interestingly, analysis of the optimal control from simulations emphasized gradual elimination of the infection in the population and finally flattens the transmission curve and so health practitioner and concerned authorities are better educated about possible control measures and the overall combine effects of such measures.

Keywords: Fractional Order; Diphtheria; Control Strategies; Fractional derivative; Positivity; Adam's Bahforth;
2020 Mathematics Subject Classification: 37N25; 93A30
Receive: 12 June 2024, **Accepted:** 12 October 2024

1 Introduction

The deadly viral illness diphtheria is brought on by a bacteria called Corynebacterium diphtheriae, which produces a toxin that destroys the cells in the human body, Medications and antitoxin drugs for diphtheria are used to treat diphtheria sickness because they both kill the germs and stop them from harming bodily tissues [7],[20],[21]. Usually, two to five days after being exposed to the germs, symptoms appear. The severity of the symptoms varies. In the moderate stage, symptoms include temperature and sore throat; in the more serious stage, symptoms include difficulties with swallowing and inhaling as well as a barking cough. Additionally, there is a chance of kidney-related issues, cardiac muscle and nerve damage, and swelling [28],[24],[17]. Therefore, it is advised that those who are affected get treatment in order to help avert devastating consequences. Humans can get diphtheria through indirect interactions with infected clothing and items or by coughing and sneezing into infected droplets of air [24]. People

[1]Corresponding author: Department of Mathematics, College of Science and Information Technology, Tai Solarin University of Education, Ogun State. NIgeria, Email: loyinmiac@tasued.edu.ng
[2]Department of Mathematics college of physical science, Federal university of agriculture Abeokuta, Ogun State Nigeria, Email: ijaolaal@funaab.edu.ng

can get the infection from an asymptomatic carrier for up to four weeks[17]. Timely administration of recommended vaccinations provides the best defense against diphtheria [6]. During adolescence and young adulthood, three additional doses of the diphtheria toxoid vaccination should be administered. Thus, it is important to inform parents about the advantages of being immunized on a regular basis to avoid diphtheria [17],[21],[22]. Finding a workable plan, policy, or strategy to get a system to its best potential conclusion is known as an optimum control. This concept helps to reduce the number of afflicted persons as it aims at maximizing the objective function. Hence, the results of several writers' applications of the principles of optimum control to infectious diseases such as trypanosomiasis[11], prevention of tobacco use [26]. Prevention of Covid-19 transmitted through contaminated surfaces and the likes [5],[12],[13]. Typhoid infection[23], Measles and Nipah virus[10], [22] and diphtheria[15] are beneficial in the management of these illnesses. Significant insights into the dynamics of infectious disease transmission, epidemiological processes, and the application of control methods may be gained from mathematical representations of infectious illnesses [1],[2], [20],[22],[25]. It may also be used to help regulators comprehend and foresee how an infectious illness will behave in a variety of settings [27],[30]. Numerous writers such as in[14] have examined the disease's behavior without taking into account the polluted surroundings and this is crucial to the spread of the diphtheria bacterium. Some modelers such as in[16] examined the effect of vaccination on diphtheria illness in a subpopulation of humans without taking into account the quantity of bacteria in the environment (the "Bacteria segment"). While analyzing for optimal control for diphtheria transmission dynamics, the above modelers only considered the effect of vaccination on diphtheria disease transmission neglecting the influence of booster doses and the rate of bacterial divisions, significant parameters that influence the dynamics of diphtheria [3].

1.1 Motivation of this study

Literatures have demonstrated efficient deterministic models in the transmission dynamics of diphtheria and many infectious disease and the analysis of optimal control measures for them, we want to further study the transmission of diphtheria and, for the first time test the effects of the combination of two control measures – Public awareness (U_1) and immediate treatment after being diagnosed (U_2) using fractional derivatives of SEIR epidemic model. We believe relevant health policy makers and agencies will benefit from our results that confirms the effectiveness of these control measures and their combination on the transmission dynamics of diphtheria.

1.2 The article's arrangement

Section 2 contains some established results needed for the study. In 2.2, we constructed a fractional model for Diphtheria and necessary qualitative analysis was done to validate the model. Adams Bashforth estimator-predictor method was used for the numerical analysis of the model and thereafter the findings from the results were discussed. MATLAB software was used for the numerical simulation. Section 3 discussed the concluding part of the study.

1.3 Materials

This section includes some notations, definitions, and established results that are required for the sequel. This study uses Liouville-Caputo's fractional derivative.

Definition 1.1. *Let J be a Real Function in the range $C_\chi, where \chi \in R, t > 0$, if $n > \chi$, then*

$$J(t) = t^n k(t) \tag{1.1}$$

where, $K \in C[0, \infty]$, and its said to be in the range C_χ^m if and only if $J^{(m)} \in C_\chi, m \in M$.

Definition 1.2. *The Transformation of Laplace is given by [19]*

$$F(s) = L\{F(t)\}(s) = \int_0^\infty e^{-st} F(t)dt \tag{1.2}$$

Where $F(t)$ is function to be transformed.

Definition 1.3. *The fractional Integrating operator of order $\alpha \geq 0$, of the Riemann Liouville of function $J \in L^1(a,b)$ defined by [19]*

$$I^\alpha J(t) = \frac{1}{\Gamma(\alpha)} \int_0^t (t-\tau)^{\alpha-1} J(\tau)d\tau \tag{1.3}$$

for $t > 0, \alpha > 0$, where Γ is the function Gamma and$I^0 J(t) = f(t)$.

Definition 1.4. *The Fractional Derivative in the Caputo sense is given by [19].*

$$D^\alpha u(t) = I^{n-\alpha} D^n J(t) = \frac{1}{\Gamma(n-\alpha)} \int_0^t (t-\tau)^{n-\alpha-1} J^{(n)}(\tau)d\tau \tag{1.4}$$

where $n \in N$ and $n-1 < \alpha \leq n$ for $t > o$

Definition 1.5. *The Mittag-Leller generalized function also known as two Parameter function is given by [19].*

$$E_{\alpha,\beta}(z) = \sum_{k=0}^{\infty} \frac{z^k}{\Gamma(\alpha k + \beta)} \tag{1.5}$$

$\mathrm{Re}(\alpha) > 0$, $\beta, Z \in C$, *When $\beta = 1$ the mittag-leffler function with one parameter is derived as a particular instance of this function and is denoted as;*

$$E_{\alpha,\beta}(z) = E_{\alpha,1}(z) = \sum_{k=0}^{\infty} \frac{z^k}{\Gamma(\alpha k + 1)}$$

for $\mathrm{Re}(\alpha) > 0$ *and $Z \in C$*
α and β can as well take any form of different values in other to show that the Mittag-Leffler function can represent important special cases.

Lemma 1.6. *for $\mu > 0$ and $0 < \alpha \leq 1$ hence the function $E_{\alpha,\beta}(-\mu z^\alpha)$, $\alpha \leq \beta$ is monotonically decreasing positive function of $z > 0$ [19]*

Definition 1.7. *For the Liouville-Caputo's derivative its Laplace transform is given by [19],[29].*

$$L\{D^\alpha N(t)(s)\} = S^\alpha N(s) + \sum_{k=0}^{n-1} S^{n-k-1} N^k(0), \quad \mathrm{Re}(\alpha) > 0, \quad (n-1) < \alpha \leq n \tag{1.6}$$

Lemma 1.8. *Putting into consideration the two parameters of Mittag-Leffler function then we have the Laplace transform formula by[19].*

$$L\{x^{\beta-1} E_{\alpha,\beta}(\mu^* t^\alpha)\}(s) = \frac{s^{\alpha-\beta}}{s^\alpha - \mu^*} \tag{1.7}$$

where $\mathrm{Re}(z) > 0$ *and* $\alpha, \beta, \mu^* \in C$

Lemma 1.9. *let* $\Psi \in C[a,b]$ *and* $D^{\alpha}\Psi \in (0,b]$ *let* $0 < \alpha \leq 1$, *therefore we have [19]*

$$u(t) = u(\alpha) + \frac{1}{\Gamma(\alpha)} D^{\alpha} u(\chi)(t-a)^{\alpha}$$

for $0 \leq \chi \leq t$ *where* $t \in (a,b]$

The Above Lemma is Mean Value Theorem which is the generalized one.

Lemma 1.10. *for* $J \in C[x,y]$ *and* $D^{\alpha}J \in (x,y]$ *let* $0 < \alpha \leq 1$, *hence the we have the following [19].*
(a) $D^{\alpha}J(t) \geq 0, \forall t \in (0,y)$ *then the function* J *is increasing*
(b) $D^{\alpha}J(t) \leq 0, \forall t \in (0,y)$ *then the function* J *is decreasing.*

2 Method

In this session, we present a system of time-fractional order to further comprehend the disease's transmission based on the previously provided information and to study the effects of some important measures: public awareness (U_1), immediate and adequate treatment after being diagnosed (U_2) which include vaccination and the combination of two control (U_3).

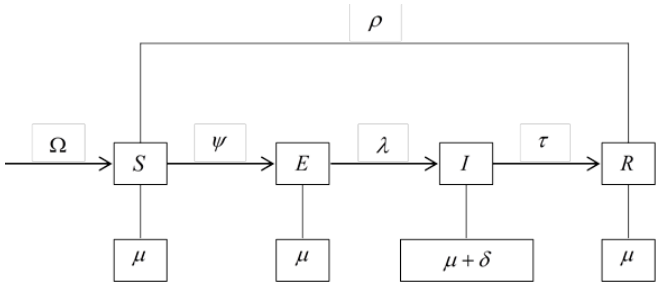

Figure 1: the diagrammatic flow of the modified Diphtheria Model.

2.1 Model Formulation

We created a compartmental diphtheria model in this section, where people/individuals are categorized as susceptible (S), exposed (E), infected (I), and recovered (R) at time t. The force of infection used was denoted as; $\Psi = \frac{\beta I}{1+aI}$, Where β is the contact rate of the disease a is the saturation factor. The results acquired for this research reveal that the saturation rates and forces of infection above project the dynamical behavior of the model when I get very high in the population as well as their inhibitory effects when simulated. Because of this, the specific saturation incidence rate has been taken into account for this model.

2.2 The Diphtheria Model Equations

The set of time fractional differential equations designed to describe the dynamics of the disease is based on the underlying assumptions of the above Model 1.

$$\left.\begin{array}{c} D^{\alpha}S(t) = \Omega - (\psi+\mu)S + \rho R \\ D^{\alpha}E(t) = \psi S - (\mu+\lambda)E \\ D^{\alpha}I(t) = \lambda E - (\tau+\mu+\delta)I \\ D^{\alpha}R(t) = \tau I - (\mu+\rho)R \end{array}\right\} \tag{2.1}$$

with the initial condition;

$$S(0) \geq 0, \;\; E(0) \geq 0, \;\; I(0) \geq 0 \;\; and \;\; R(0) \geq 0 \tag{2.2}$$

here $D^{\alpha} = \frac{d^{\alpha}}{dt^{\alpha}}$ for $0 < \alpha \leq 1$ in the Liouville-Caputo Fractional derivative of order α
The following includes the state variables and parameter descriptions

Table 1: Parameters and Description.

parameters	Description
Ω	Recruitment/Immigration rate
β	Contact rate of the disease
μ	Natural death rate
λ	Progression rate I
τ	Recovery rate
δ	Death caused by the disease
ρ	Relapse rate
N	The Total Population

2.3 Qualitative Analysis of the proposed Fractional Model.

To demonstrate the uniqueness and existence of solutions to the system under consideration in 2.1 and 1.10 as it has been given above is required, which given as;

Lemma 2.1. *for $J \in C[x,y]$ and $D^{\alpha}J \in (x,y]$ let $0 < \alpha \leq 1$, hence the we have the following [19].*
(a) $D^{\alpha}J(t) \geq 0, \forall t \in (0,y)$ then the function J is increasing
(b) $D^{\alpha}J(t) \leq 0, \forall t \in (0,y)$ then the function J is decreasing.

The proof of the above lemma is direct consequence of lemma 1.9 which is the generalized Mean Value Theorem.

2.4 Boundedness and Positivity of Solution

This section shows that the variables that represent the population compartments stay non-negative (positive) throughout the simulation. Furthermore, we prove that the population as a whole stays constant and that the number of people in each compartment never rises above the size of the entire population. The total human population is given as;

$$N(t) = S(t) + E(t) + I(t) + R(t). \tag{2.3}$$

which was translate to fractional form as

$$D^{\alpha}N(t) = D^{\alpha}S(t) + D^{\alpha}E(t) + D^{\alpha}I(t) + D^{\alpha}R(t) \tag{2.4}$$

$$D^{\alpha}N(t) = \Omega - \mu S - \mu E - \mu I - \mu R \tag{2.5}$$
$$= \Omega - \mu(S + E + I + R) \tag{2.6}$$
$$D^{\alpha}N(t) = \Omega - \mu N \tag{2.7}$$

Theorem 2.2. *Let be the solution to the Diphtheria model equation 2.1 in a physiologically viable area* $\wedge$

where

$$\Lambda = (S, E, I.R) \in R_{+}^{4} : N \leq \frac{\Omega}{\mu}$$

Proof. With the Laplace transform applied on both sides of 2.7, and using the definition as listed in 1.7 we have

$$S^{\alpha}N(s) + S^{\alpha-1}N(0) = \frac{\Omega}{s} - \mu N(s) \tag{2.8}$$

on rearranging 2.8 we have

$$N(s) = \frac{\Omega}{s(s^{\alpha} + \mu)} + \frac{s^{\alpha-1}}{s^{\alpha} + \mu}N(0) \tag{2.9}$$

After considerable simplification and application of the Laplace inverse transform and 1.8 on 2.9 the following was obtained

$$N(t) = N(0)E_{\alpha}(-\mu t^{\alpha}) + \frac{\Omega}{\mu}[1 - E_{\alpha}(-\mu t^{\alpha})] \tag{2.10}$$

on using 2.10 with 1.6, as $t \to \infty$ we have

$$N(t) \leq \frac{\Omega}{\mu} \tag{2.11}$$

hence $\wedge$ is bounded. Thus, every solution for systems 2.1 and is included inside the set. □

Hence, from equation2.8 to 2.11, we have verified that the solutions for the various compartments are bounded and that the model is well-posed both mathematically and epidemiologically.

2.5 Positivity of Solution

For all time $t > 0$, the model's solution in system 2.1 with positive initial conditions will continue to be non-negative

Proof. Using the Mittag-Leffter function also known as two parameter function

$$E_{\alpha,\beta} = \sum_{k=0}^{\infty} \frac{(Z)^{k}}{\Gamma\alpha k + \beta} \tag{2.12}$$

Replacing Z with our population $N(t)$ and $k = 0, 1, 2, \ldots$ with $\alpha = \beta = 1$, we have

$$E_{1,1} = \sum_{k=0}^{\infty} \frac{(N(t))^{k}}{\Gamma\alpha k + \beta} = \frac{(N(t))^{0}}{\Gamma(0+1)} + \frac{(N(t))^{1}}{\Gamma(1+1)} + \ldots \tag{2.13}$$

Neglecting the higher terms on the right hand side 2.13 yields

$$E_{1,1} = \sum_{k=0}^{\infty} \frac{(N(t))^{k}}{\Gamma\alpha k + \beta} \approx \frac{1}{\Gamma(1)} + \frac{(N(t))^{1}}{\Gamma(2)} \tag{2.14}$$

recall that $\Gamma(1) = 1$

$$E_{1,1} = \frac{(N(t))}{\Gamma\alpha k + \beta} \approx 1 \tag{2.15}$$

We conclude that the set is positive for time (t) based on equations of the model 2.1 □

2.6 Basic Reproduction Number

R_0 being the diphtheria disease basic reproduction number, is a crucial epidemiological metric that indicates the likelihood of the illness spreading among a population lacking resistance/immunity. This number offers important insights into the possible severity and outbreak, so accurate calculation of this parameter is essential. By applying the well-known generation Matrix as implemented in [2]

Proof. let F be the Matrix of new infection and V be the matrix of secondary infection, so we have

$$F = \begin{bmatrix} \psi_S \\ 0 \end{bmatrix} = \begin{bmatrix} \left(\frac{\beta I}{1+aI}\right) S \\ 0 \end{bmatrix}, \quad \begin{bmatrix} \frac{\partial f_1}{\partial E} & \frac{\partial f_1}{\partial I} \\ \frac{\partial f_2}{\partial E} & \frac{\partial f_2}{\partial I} \end{bmatrix} = \begin{bmatrix} 0 & \beta S \\ 0 & 0 \end{bmatrix} \tag{2.16}$$

$$V = \begin{bmatrix} -(\mu+\lambda) E \\ \lambda_E - (\tau+\mu+\delta) I \end{bmatrix}, \quad \begin{bmatrix} \frac{\partial V_1}{\partial E} & \frac{\partial V_1}{\partial I} \\ \frac{\partial V_2}{\partial E} & \frac{\partial V_2}{\partial I} \end{bmatrix} = \begin{bmatrix} -(\mu+\lambda) & 0 \\ \lambda & -(\tau+\mu+\delta) \end{bmatrix} \tag{2.17}$$

$$|V| = (\mu+\lambda)(\tau+\mu+\delta) \tag{2.18}$$

$$Adj(V) = \begin{bmatrix} -(\tau+\mu+\delta) & 0 \\ -\lambda & -(\mu+\lambda) \end{bmatrix} \tag{2.19}$$

$$V^{-1} = \frac{Adj(V)}{|V|} = \begin{bmatrix} \frac{-(\tau+\mu+\delta)}{(\mu+\lambda)(\tau+\mu+\delta)} & \frac{0}{(\mu+\lambda)(\tau+\mu+\delta)} \\ \frac{-\lambda}{(\mu+\lambda)(\tau+\mu+\delta)} & -\frac{(\mu+\lambda)}{(\mu+\lambda)(\tau+\mu+\delta)} \end{bmatrix} \tag{2.20}$$

$$V^{-1} = \begin{bmatrix} \frac{-1}{(\mu+\lambda)} & 0 \\ \frac{-\lambda}{(\mu+\lambda)(\tau+\mu+\delta)} & \frac{-1}{(\tau+\mu+\delta)} \end{bmatrix} \tag{2.21}$$

$$R_0 = \Delta F.V^{-1} == \begin{bmatrix} 0 & \beta S \\ 0 & 0 \end{bmatrix} \begin{bmatrix} \frac{-1}{(\mu+\lambda)} & 0 \\ \frac{-\lambda}{(\mu+\lambda)(\tau+\mu+\delta)} & \frac{-1}{(\tau+\mu+\delta)} \end{bmatrix} \tag{2.22}$$

$$|FV^{-1} - \lambda I| = \begin{bmatrix} \frac{\beta S\lambda}{(\mu+\delta)(\tau+\mu+\delta)} - \lambda & \frac{\beta S}{(\tau+\mu+\delta)} \\ 0 & 0-\lambda \end{bmatrix} = \frac{\beta S\lambda}{(\mu+\delta)(\tau+\mu+\delta)} \tag{2.23}$$

$$R_0 = \frac{\beta\,\Omega\,\lambda}{\mu(\mu+\delta)(\tau+\mu+\delta)} \tag{2.24}$$

recall that at infection free, $S = \frac{\Omega}{\mu}$, therefore

$$R_0 = \frac{\beta\,\Omega\,\lambda}{\mu(\mu+\delta)(\tau+\mu+\delta)} \tag{2.25}$$

□

2.7 Stability Analysis

Using system 2.1 and model parameters, we examined the local stability of the infection-free equilibrium (IFE) for the diptheria model. In an epidemiological model, the Infection-free equilibrium is a unique position when the disease is not spreading across the population as a whole and all disease chambers are equal to zero

Theorem 2.3. *If $R_0 \leq 1$ then the fractional order model 2.1 is stable locally*

Proof.

$$DFE = \left(\frac{\Omega}{\mu}, 0, 0, 0\right), \qquad J(S, E, I, R) \tag{2.26}$$

at infection free we have the above holds

$$\left.\begin{array}{c} F_1 = \Omega - \frac{\beta SI}{1+aI} - \mu S + \rho R \\ F_2 = \frac{\beta SI}{1+aI} - \mu E + \alpha E \\ F_3 = \alpha E - (\tau + \mu + \delta) I \\ F_4 = \tau I - \mu R - \rho R \end{array}\right\} \tag{2.27}$$

using the Jacobian technique

$$J = \begin{bmatrix} \frac{\partial F_1}{\partial S} & \frac{\partial F_1}{\partial E} & \frac{\partial F_1}{\partial I} & \frac{\partial F_1}{\partial F} \\ \frac{\partial F_2}{\partial S} & \frac{\partial F_2}{\partial E} & \frac{\partial F_2}{\partial I} & \frac{\partial F_2}{\partial R} \\ \frac{\partial F_3}{\partial S} & \frac{\partial F_3}{\partial E} & \frac{\partial F_3}{\partial I} & \frac{\partial F_3}{\partial R} \\ \frac{\partial F_4}{\partial S} & \frac{\partial F_4}{\partial E} & \frac{\partial F_4}{\partial I} & \frac{\partial F_4}{\partial R} \end{bmatrix} \tag{2.28}$$

The Local Stability was calculated at disease free equilibrium
after step by step solving and simplifying the 4 by 4 jacobian Matrix (2.28) we have that Eigenvalues are all negative which are

$$\kappa_1 = -\mu, \kappa_2 = -(\mu + \rho), \kappa_3 = -\lambda, \kappa_4 =, \frac{-\lambda\beta\Omega}{\mu(\mu + \alpha)(\tau + \mu + \delta)} = R_0 \tag{2.29}$$

Clearly, $\kappa_1 = \kappa_2 = \kappa_3 = \kappa_4$ are all (negative) stable
in addition $\kappa_4 = R_0 < 1$ which shows that our model at infection free equilibrium is locally asymptotically stable. (LAS).This implies that, on an average, each sick person spreads the disease to fewer vulnerable. As a consequence, the diphtheria germs can no longer survive in the community, and as time goes on, fewer people become affected until the disease is completely eradicated. Our local asymptotic stability thus demonstrates that the system will eventually converge to point of equilibrium if it begins close to the infection-free. Hence the above theorem has been proved. □

2.8 Global Stability

Theorem 2.4. *If $R_0 \leq 1$, then model 2.1 is globally asymptotically stable.*

Proof. by implementing the method in [20], we say that $E^0 = (M^0, 0)$ is stable globally if $R_0 \leq 1$. By splitting our model 2.1 into two distinct part, that is;
$M = (S, R)$ and $J = (E, I)$ where M and J represent the uninfected and the infected population respectively
we have

$$\frac{d^\alpha M}{dt} = F(M, J) \text{ and } \frac{d^\alpha J}{dt} = G(M, J), G(M, 0) = 0$$

$$F(M,J)=\begin{bmatrix} \Omega-\psi_S-\mu_S+\rho_R \\ \tau_I-\mu_R-\rho_R \end{bmatrix}, G(M,J)=\begin{bmatrix} \psi_S-\mu_E-\lambda_E \\ \lambda_E-(\tau+\mu+\delta)I \end{bmatrix} \tag{2.30}$$

with $G(M,0)=0$, $E^0=(M^*,0)$ at DFE of the system $M^*=\left(\frac{\Omega}{\mu},\ 0\,0\,0\right)$, H_1 and H_2 need to be satisfied for global stability where H_1 : $\left(\frac{dM}{dt}\right)=F(M,0)$ and H_2 : $G(M,J)=BN-G(M,J)$ with B as a K-matrix when the non-diagonal element is positive, lets consider the system that was reduced which is; $\left(\frac{d^\alpha M}{dt}\right)=F(M,0)$ where $J=0$ is the infected class

$$F(M,0)=\begin{bmatrix} \Omega-\mu_S+\rho_R \\ -\mu_R-\rho_R \end{bmatrix},\ M^*=(S,R)=\left(\frac{\Omega}{\mu},0\right) \tag{2.31}$$

The reduced system for GAS equilibrium point is $\frac{d^\alpha M}{dt}=F(M,0)$ of (2.1) has been gotten earlier on by establishing positivity of 2.1

Hence, we got the respective value of DFE. Therefore, we conclude the convergence of the solution to our equations is globally stable on the feasible region

now to establish H_2 , we have $G(M,J)=\left[BN-\dot{G}(M,J),\dot{G}(M,J)\geq 0\ \ (M,J)\in K\right]$

$$\begin{bmatrix} \frac{\partial F_1}{dE} & \frac{\partial F_1}{dI} \\ \frac{\partial F_2}{dE} & \frac{\partial F_2}{dI} \end{bmatrix}=\begin{bmatrix} -(\mu+\lambda) & 0 \\ \lambda & -(\tau+\mu+\delta) \end{bmatrix}, \qquad J=\begin{bmatrix} E \\ I \end{bmatrix} \tag{2.32}$$

Clearly all the diagonal entries of B are negative which conveys stability. Hence

$$\dot{G}(M,J)=\left[\Psi\left(\frac{\Omega}{\mu}-S\right)\right] \tag{2.33}$$

Hence, we have verified the global stability of the model (2.1) □

2.9 Endemic Equilibrium State

The occurrence of endemic equilibrium points; this is the stable state solutions in the model when the diphtheria disease is continuously present in the population is examined, in this stage. The stable disease states at which the proportion of sick people and other components attain a steady state are represented by these equilibrium points. By setting the temporal derivatives of the model variables to zero and solving the ensuing system of equations, we may mathematically determine the endemic equilibrium state. These points offer crucial insights into the long-term dynamics of the disease epidemic in the population as they reflect the stable solutions of the model where the disease endures throughout time.

$$\left.\begin{array}{ll} D^\alpha S(t)=D^\alpha E(t)=D^\alpha I(t)=D^\alpha R(t)=0 & \\ \Omega-\psi S-\mu S+\ell R=0 & (i) \\ \psi S-\mu E-\lambda E=0 & (ii) \\ \alpha E-(\tau+\mu+\delta)I=0 & (iii) \\ \tau I-\mu R+\ell R=0 & (iv) \end{array}\right\} \tag{2.34}$$

The resulting solutions from (2.34) yields;

$$E^*=\{S^*,E^*,I^*,R^*\}=\left\{\begin{array}{l} \frac{\Omega}{(\Psi+\mu)(\mu+\lambda)^2(\tau+\mu+\delta)^2(\mu+\rho)^2(\rho\tau\lambda\Psi)} \\ \frac{\Psi S}{(\mu+\lambda)} \\ \frac{\lambda\Psi S}{(\mu+\lambda)(\tau+\mu+\delta)} \\ \frac{\tau\lambda\Psi S}{(\mu+\lambda)(\tau+\mu+\delta)(\mu+\rho)} \end{array}\right\} \tag{2.35}$$

Showing that the endemic equilibrium state exist

2.10 Optimal Control Analysis

The following are essential elements of the best tactics/strategies against the diphtheria virus: We minimize costs while optimizing output when we lower the transmission rate by $(1-U_1)$, where U_1 denotes launching public awareness campaigns in affected regions to boost immunity in the population instead of Vaccination, especially in the susceptible class, and lower the risk of Diphtheria outbreaks; U_2 denotes intervention, such as vaccination, and other potential measures for both exposed and sick individuals(treatment in general); U_3 is the combination of these measures to lessen the intensity of outbreaks.
recall that $\psi = \frac{\beta SI}{1+aI}$ and $0 < \alpha \leq 1$, let $\alpha = 1$ for simplicity.

$$\left.\begin{array}{c} U_1 = Public\ Awareness \\ U_2 = Treatment \\ U_3 = Combination\ of\ U_1\ and\ U_2 \end{array}\right\}$$

Let σ be the probability of infection, the D.E becomes

$$\left.\begin{array}{l} D^{\alpha}S(t) = \Omega - \frac{(1-U_1)\,\sigma\beta IS}{1+aI} - \mu S + \rho R \\ D^{\alpha}E(t) = \frac{(1-U_2)\,\sigma\beta SI}{1+aI} - \mu E + \lambda E \\ D^{\alpha}I(t) = \lambda E - (\tau + \mu + \ell)\, I - U_3 I \\ D^{\alpha}R(t) = U_3 I + \tau I + \mu R - \rho R \end{array}\right\} \tag{2.36}$$

2.10.1 Qualitative Analysis of the Model with Control Measure

A function with an objective is created using Pontryagin's maximal principle, and we show that the objective function (H) has an optimal control, which identifies the most successful control method; Analysis shows that increasing public awareness U_1, providing treatment (vaccine and other potential information from appropriate government or private entities), U_2 and combining these strategies U_3 will reduce the spread of this fatal sickness within a certain amount of time in the internal
$\left[0, \bar{1}\right]$ and $U = \{(U_1, U_2, U_3 \in U)\}$ Lebesgue measurable on $[0,1]$, $0 \leq U_i(t) \leq 1 \in [0,1]$, $i = 1,2,3.$
The objective functional (H) is defined as follows:

$$H\left(U_1, U_2, U_3\right) = \int_0^T \left(M_1 I + M_2 E + \frac{1}{2}\left(\omega_1 M_1^2 + \omega_2 M_2^2\right) + \omega_3 M_3^2\right) dt \tag{2.37}$$

Which is subject to;

$$H\left(U_1^*(t), U_2^*(t), U_3^*(t)\right) = Min\left\{H\left(U_1, U_2, U_3\right), \qquad U_1, U_2, U_3 \in k\right\} \tag{2.38}$$

2.10.2 Presence of an Optimal Control

Theorem 2.5. *on using the objective functional $H\left(U_1, U_2, U_3\right)$ as in when the measure set U is measurable subjected to the starting points given as t tends towards zero there exists an optimal control $U^* = \left(U_1^*(t),\ U_2^*(t),\ U_3^*(t)\right)$ such that*

$$H\left(U_1^*(t),\ U_2^*(t),\ U_3^*(t)\right) = \min\left\{H\left(U_1,\ U_2\ \ U_3\right),\ \ U_1,\ U_2\ \ U_3 \in k\right\} \tag{2.39}$$

Proof. The Lipschitz property of the system of the model concerning with regard to the state of variables S, E, I, and R, the boundedness of the solution, and the integral convexity of (H) to optimize control U_1, U_2, and U_3 lead to the existence of the optimal central of the model.
Let's now determine the Hamilton H and the Lagrangian L for the optimum control issue. The Lagrangian

is as follows;

$$L = M_1 I + M_2 E + \frac{1}{2}\left(W_1 U_1^2 + W_2 U_2^2 + W_{3\backslash} U_3^2\right) \tag{2.40}$$

and the Hamiltonian given as follows;

$$\left.\begin{array}{c} H = M_1 I + M_2 E + \frac{1}{2}\left(W_1 U_1^2 + W_2 U_2^2 + W_{3\backslash} U_3^2\right) \\ +\alpha_{\overline{1}} S\left[\Omega - \frac{(1-U_1)\sigma\beta SI}{1+aI} - \mu S + \rho R\right] \\ +\alpha_{\overline{1}} S\left[\frac{(1-U_2)\sigma\beta SI}{1+aI} - \mu S - \lambda E\right] \\ +\alpha_{\overline{1}} I\left[\lambda E - (\tau+\mu+\delta) I - U_3 I\right] \\ +\alpha_{\overline{1}} R\left[U_3 I + \tau I - \mu R - \rho R\right] \end{array}\right\} \tag{2.41}$$

where $\alpha\tau_I,\ i \in (S, E, I, R)$ are the disjointed variables, We apply the required conditions to the Hamiltonian in the above Theorem □

Theorem 2.6. *Considering an optimal control* $U^* = (U_1^*(t), U_2^*(t), U_3^*(t))$ *and a solution* $Z^* = \{S^*, E^*, I^*, R^*\}$ *of the existing model (2.1), then there exist an adjoint variable* $i \in \{S^*, E^*, I^*, R^*\}$ *satisfying*

$$\left.\begin{array}{c} \frac{d\alpha_{\overline{\eta}} S}{dt} = \left[\alpha_\tau S\left(-\frac{(1-U_1)\beta I}{1+aI} - \mu + \alpha_{\overline{1}} E\left(\frac{(1-U_1)\beta I}{1+aI}\right)\right)\right] \\ \frac{d\alpha_{\overline{\tau}} e}{dt} = \left[M_2 + \alpha_{\overline{1}} E\left((\mu+\alpha) - \alpha_{\overline{1}} I\alpha\right)\right] \\ \frac{d\alpha_{\overline{1}} I}{dt} = \left[M_1 + \alpha_\tau S\left(-\left(1-U_1\right)\sigma\beta S + \alpha_{\overline{1}} E\left(\frac{(1-U_2)\sigma\beta S}{(1+aI)^2}\right)\right)\right] \\ +\alpha_\tau I\left(\tau + (\mu+\delta) - U_3\right) + \alpha_\eta R\left(U_3 + \tau\right) \\ \frac{d\alpha_{\overline{1}} R}{dt} = -\alpha_{\overline{1}} R\left(+\left(\mu - \rho\right)\right) \end{array}\right\} \tag{2.42}$$

Proof. With transversality condition $\alpha_{\overline{i}} S\left(\overline{1}\right) \in \{S, E, I, R\}$, which implies the control objectives are

$U_1^* = \min\{1, \max\{0, y_1\}\}\quad U_2^* = \min\{1, \max\{0, y_2\}\}\quad U_3^* = \min\{1, \max\{0, y_3\}\}$
We differentiate the Hamiltorian with respect to the state variables and obtain the following equation

$$\left.\begin{array}{c} \frac{d\alpha_{\overline{1}} S}{dt} = \frac{\partial H}{dS} = \left[\alpha_{\overline{1}} S\left(-\frac{(1-U_1)\beta I}{1+aI} - \mu + \alpha_{\overline{1}} E\left(\frac{(1-U_1)\beta I}{1+aI}\right)\right)\right] \\ \frac{d\alpha_{\overline{1}} e}{\partial t} = -\frac{\partial H}{dE} = -M_2 + \left[\alpha_{\overline{1}} E\left(+(\mu+\alpha) - \alpha_{\overline{1}} I\alpha\right)\right] \\ \frac{d\alpha_{\overline{1}} I}{dt} = -\frac{\partial H}{\partial I} = M_1 + \alpha_{\overline{1}} S\left(-\left(\frac{(1-U_1)\sigma\beta S}{(1+aI)^2}\right) + \alpha_{\overline{1}} E\left(\frac{(1-U_1)\sigma\beta S}{(1+aI)^2}\right)\right) \\ +\alpha_{\overline{1}} I\left(\tau + (\mu+\delta) - k_3\right) + \alpha_{\overline{1}} R\left(k_3 + \tau\right) \\ \frac{d\alpha_{\overline{1}} R}{dt} = -\frac{\partial H}{\partial R} = \left[-\alpha_{\overline{1}} R\left(+(\mu-\rho)\right)\right] \end{array}\right\} \tag{2.43}$$

With the transversality condition $\alpha_{\overline{i}} S\left(\overline{1}\right) \in \{S, E, I, R\}$ to simplifies the Hamiltonian H with regards to the control options, thus H is differentiated with respect to U_1, U_2 and U_3 we have

$$\left.\begin{array}{l} W_1 U_1 + \left(-\alpha_{\overline{1}} S\left[\frac{\sigma\beta SI}{1+aI}\right] + \alpha_{\overline{1}} E\left(\left[\frac{\sigma\beta SI}{1+aI}\right]\right)\right) = 0 \\ W_1 U_1 = \frac{\sigma\beta SI\left(\alpha_{\overline{1}} E - \alpha_{\overline{1}} S\right)}{1+aI} \\ U_1^* = \frac{\sigma\beta SI\left(\alpha_{\overline{1}} E - \alpha_{\overline{1}} S\right)}{W_1(1+aI)} \end{array}\right\} \tag{2.44}$$

$$\left.\begin{array}{l} W_2 U_2 - \alpha_{\overline{1}} E\left(\frac{\sigma\beta SI}{1+aI}\right) \Rightarrow U_2 = \frac{\alpha_{\overline{1}} E\sigma\beta SI}{W_2(1+aI)} \\ U_2^* = \frac{\alpha_{\overline{1}} E\sigma\beta SI}{W_2(1+aI)} \end{array}\right\} \tag{2.45}$$

$$\left.\begin{array}{l} W_3U_3 - \alpha_{\overline{1}} I\,(-I) + \alpha_{\overline{1}} R\,(I) \\ W_3U_3 = \frac{I\left(\alpha_{\overline{1}} I - \alpha_{\overline{1}} R\right)}{W_3} \\ U_3^* = \frac{I\left(\alpha_{\overline{1}} I - \alpha_{\overline{1}} R\right)}{W_3} \end{array}\right\} \tag{2.46}$$

$$\eta_1 = \frac{\sigma\beta SI\,(\alpha_{\overline{1}} E - \alpha_{\overline{1}} S)}{W_1\,(1+aI)}, \eta_2 = \frac{\alpha_{\overline{1}} E\sigma\beta SI}{W_2\,(1+aI)}, \eta_3 = \frac{I\,(\alpha_{\overline{1}} I - \alpha_{\overline{1}} R)}{W_3} \tag{2.47}$$

Thus, we have been to establish the conditions for presence of optimal Measure (control □

2.11 Numerical Solution for the fractional Order Model 2.1 in the sense of Caputo derivative

We apply the Caputo fractional operator to study the dynamics of the proposed fractional-order model. The proposed nonlinear fractional-order system's numerical simulation is provided by the Adams type estimator-corrector approach [30],[9]. We consider the Cauchy-type FDE with respect to the order α Caputo operator.
$D_t^\alpha X(t) = \Pi(t, x(t)), \quad X^{(i)}(0) = X_0^i, \quad 0 < \alpha \leq 1$
where $i = 0, 1, 2...n-1$, the above condition can be transformed to Voltera equation of the form

$$X(t) = \sum_{i=0}^{n-1} X_0^{(i)} \frac{t^i}{i!} + \frac{1}{\Gamma(\alpha)} \int_0^t (t-s)^{\alpha-1} X(s, X(s)) ds \tag{2.48}$$

This estimated-corrector method is being proposed with respect to the algorithm of Adams Bashforth-Moulten, we make the step size to be $b = \frac{\gamma}{N}, \quad t_e = eh, \quad e = 0\,, 1,\ 2...N \in Z^+$ and $X_e \approx X(t_e)$
which can be discretize to equal equation [16]

$$\left.\begin{array}{l} S_{n+1} = \sum\limits_{e=0}^{n-1} S_0^{(e)} \frac{t_{n+1}^e}{e!} + \frac{b^\alpha}{\Gamma(\alpha+2)} \sum\limits_{e=0}^{n} (M_{e,n+1})(\Omega - (\psi+\mu)S_e + \rho R_e) \\ + \frac{b^\alpha}{\Gamma(\alpha+2)} \sum\limits_{e=0}^{n} (M_{e+1,e+1})(\Omega - (\psi+\mu)S_{n+1}^{EF} + \rho R_{n+1}^{EF}) \\ E_{n+1} = \sum\limits_{e=0}^{n-1} E_0^{(e)} \frac{t_{n+1}^e}{e!} + \frac{b^\alpha}{\Gamma(\alpha+2)} \sum\limits_{e=0}^{n} (M_{e,n+1})(\psi S_e - (\mu+\lambda)E_e) \\ + \frac{b^\alpha}{\Gamma(\alpha+2)} \sum\limits_{e=0}^{n} (M_{e+1,e+1})(\psi S_{n+1}^{EF} - (\mu+\lambda)E_{n+1}^{EF}) \\ I_{n+1} = \sum\limits_{e=0}^{n-1} I_0^{(e)} \frac{t_{n+1}^e}{e!} + \frac{b^\alpha}{\Gamma(\alpha+2)} \sum\limits_{e=0}^{n} (M_{e,n+1})(\lambda E_e - (\tau+\mu+\delta)I_e) \\ + \frac{b^\alpha}{\Gamma(\alpha+2)} \sum\limits_{e=0}^{n} (M_{e+1,e+1})(\lambda E_{n+1}^{EF} - (\tau+\mu+\delta)I_{n+1}^{EF}) \\ R_{n+1} = \sum\limits_{e=0}^{n-1} R_0^{(e)} \frac{t_{n+1}^e}{e!} + \frac{b^\alpha}{\Gamma(\alpha+2)} \sum\limits_{e=0}^{n} (M_{e,n+1})(\tau I_e - (\mu+\rho)R_e) \\ + \frac{b^\alpha}{\Gamma(\alpha+2)} \sum\limits_{e=0}^{n} (M_{e+1,e+1})(\tau I_{n+1}^{EF} - (\mu+\rho)R_{n+1}^{EF}) \end{array}\right\} \tag{2.49}$$

where

$$M_{e,n+1} = \begin{cases} n^{\alpha+1} - (n-\alpha)(n+1)^\alpha \\ (n-e+2)^{\alpha+1} + (n-e)^{\alpha+1} - 2(n-e+1)^{\alpha+1} \\ 1 \end{cases} \tag{2.50}$$

the above condition hold if $e = 0 \quad , 1 \leq e \leq n \quad$ and $\quad e = n+1$
The next stage is to create the concurrence estimator (predictor) formula. X_{n+1}^{EF} the suggested predictor

formula may be calculated as;

$$\left.\begin{aligned} S_{n+1}^{EF} &= \sum_{e=0}^{n-1} S_0^{(e)} \frac{t_{n+1}^e}{e!} + \frac{b^\alpha}{\Gamma(\alpha+1)} \sum_{e=0}^{n} (j_{e,n+1})(\Omega - (\psi+\mu)S_e + \rho R_e) \\ E_{n+1}^{EF} &= \sum_{e=0}^{n-1} E_0^{(e)} \frac{t_{n+1}^e}{e!} + \frac{b^\alpha}{\Gamma(\alpha+1)} \sum_{e=0}^{n} (j_{e,n+1})(\psi S_e - (\mu+\lambda)E_e) \\ I_{n+1}^{EF} &= \sum_{e=0}^{n-1} I_0^{(e)} \frac{t_{n+1}^e}{e!} + \frac{b^\alpha}{\Gamma(\alpha+1)} \sum_{e=0}^{n} (j_{e,n+1})(\lambda E_e - (\tau+\mu+\delta)I_e) \\ R_{n+1}^{EF} &= \sum_{e=0}^{n-1} I_0^{(e)} \frac{t_{n+1}^e}{e!} + \frac{b^\alpha}{\Gamma(\alpha+1)} \sum_{e=0}^{n} (j_{e,n+1})()\lambda E_e - (\tau+\mu+\delta)I_e \end{aligned}\right\} \tag{2.51}$$

$$\text{where } j_{e,n+1} = (n+1-e)^\alpha - (n-e)^\alpha$$

2.12 Numerical Simulation

Table 2: Initial values of the proposed population and their sources

parameters	Values	source
S	3850	UNICEF Nigeria
E	2500	Assumed
I	1387	UNICEF Nigeria
R	0	Assumed

Table 3: Parameter values used in the simulations and their source.

parameters	Values	Source
Ω	1.497	Fitted
β	0.0003465	Fitted
μ	0.10	Fitted
λ	0.030	Fitted
τ	0.01710615	Fitted
δ	0.09113	Fitted
ρ	0.0030	Fitted

3 Discussion of Findings

In this section, we provide a way to monitor and discuss changes in several parameters, assess the efficacy of strategies presented, and observe how the disease develops over time. This section might be of great help to public health officials to gain important insight into how effective the control strategies on the transmission dynamics of diphtheria and how its transmission behaves in various settings. The values in tables 2 and 3 are used for the simulations and the extended Adams-Bashforth Moulton type predictor-corrector technique is used to obtain approximate solutions for our fractional ordered model using MATLAB software 2018. Time series solutions of the system 2.1 with varying values of α are obtained using the same

parameters in 2.12 and 2.12 (refer to Figure 8, 9, 10, 11 for the simulated results.

figure 2 shows the dynamics (behavior) of the disease within the population by varying the infection rate β. The susceptible class obviously becomes more vulnerable to the disease at higher infection rates which in essence affects the exposed and infected populations. The goal of this study is to achieve a disease-free community which is only possible by employing all available tactics.
In figure 3, given the dynamic nature of the SEIR models, we assume that the population is already afflicted with the disease prior to control measure implementation. The graph demonstrated how individuals that were exposed to the disease went on to get infected over time with the susceptible population progressively declining. Additionally, increase in the rate of infection coupled with the model's assumption of immunity loss contributed to the low recovery rate. This implies the disease tends to endemic state.

In figure 4,the consistency shown in the susceptible class suggests that a greater number of people are taking precaution based on public awareness campaigns of the disease. This is a positive indication that a greater proportion of the populace is developing resistance against diphtheria by means of precaution and outbreak of Furthermore, figure 4 demonstrates that the public awareness campaign is the most successful of our methods followed by treatment (in this case, early testing because certain individuals have asymptotic traits). If the susceptible class gains stability, fewer people will be exposed, and the same is true for those who are infected (sick). Overall, results indicates that the population-wide spread of the disease will be stopped by our management measures

Figure 5 illustrates how the reduction in the exposed class suggests that the use of U_2 which is treatment (vaccination and other therapies), is successful in lowering the number of individuals who are exposed to diphtheria. This is a good result since it shows that the population is less affected by sickness. The decrease in the exposed class indicates that the population's exposure to diphtheria has been effectively reduced by this study technique. Campaigns for public awareness aid in building resistance, and integrating U_3 ,which is the combination of awareness and treatment, eventually terminates the spread of the disease. Public health benefits from the reduction in the number of exposed people. It implies a decrease in mortality as fewer individuals will become infected.

According to figure 6, our combined tactics U_3 produced a reduction in diphtheria-related mortality in the infected class. The reduction of the infected class shows that these control methods were able to achieve highlights the significance of prompt and proactive intervention tactics. Preventing major epidemics requires public awareness and treatment (vaccination and other therapies). In conclusion, Figure 6 demonstrates that treatment and public awareness initiatives can effectively lower the number of cases of diphtheria among the afflicted(infected) community by lowering the diphtheria burden, these control techniques are successful in slowing the disease's spread and enhancing overall health results.

In figure 7, over the course of 100 days, the recovered class made a significant change at first which later increases over the prescribed time. Because the individuals in this class have experienced being exposed to, infected with, and then recovered from the disease, it appears that public awareness campaigns is successfully building population resistance in this category of individuals. The next step is for them to be aware of disease in order to avoid becoming a victim of it again, which will allow us to achieve the disease-free equilibrium that is achievable under all circumstances by effectively implementing other strategies prescribed in this paper. As a consequence, more people recover from diphtheria more rapidly.

Figure 12 and 13 respectively demonstrate the dynamical behavior of the exposed and the infected class respectively when saturation is incorporated, that is, the impact of infection would be reduced coming from the incidence rate according to the line curves in this figures, in other word we are not likely

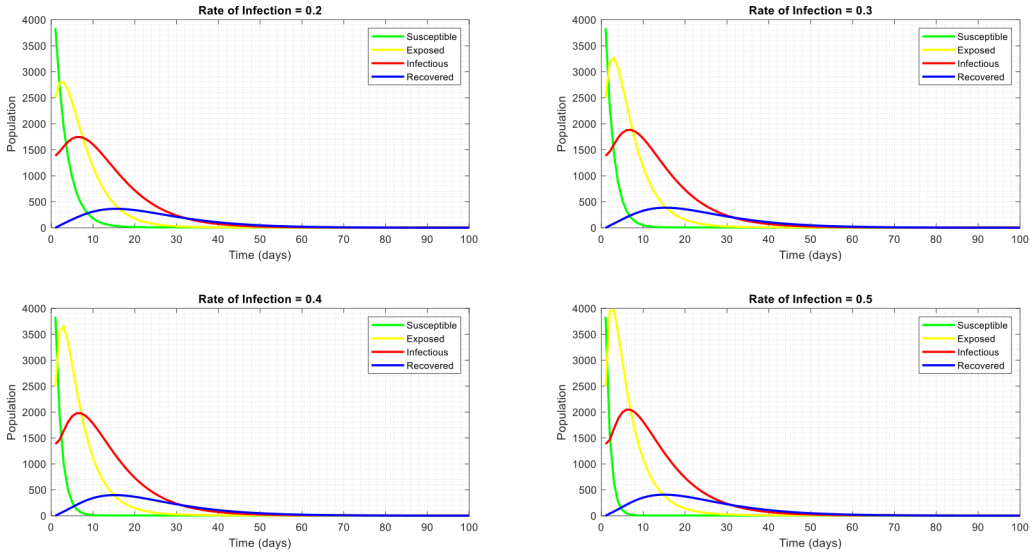

Figure 2: Effects of varying the infection rate β on the population Dynamics

to have diphtheria severity.

3.1 Conclusion

The fractional order SEIR model presented perfectly replicates the conventional system of ordinary differential equations model in literature. Although more computationally intensive, the fractional order approach is appropriately reliable due to the non-locality and its memory effect. The necessary qualitative and mathematical analysis was done to validate the model, in the same vein the study was able to establish all parameters necessary for the feasibility of the proposed model which are proven to be analytically true and also valid numerically. Approximate solutions was derived using the Adam's Bashforth predictor-Corrector scheme. Additionally, results from simulations confirm the positive effects of the combinations of the control techniques in flattening the transmission curve of the infection in the final analysis.

Figure 8, 9, 10 and 11 illustrates the constantly changing complexity of the fractional differential equations, highlighting their enhanced capability as descriptors for biological phenomena in comparison to the ordinary differential equations models. Additionally, the model's solutions, which depend on the continuously changing time-fractional derivative, consistently converge to equilibrium points which in turns aid the stability in each simulated compartments.

3.2 Suggestion for future study

We intend to extend the mathematical framework of the current study on diphtheria, to include parameter estimation, sensitivity analysis of the Reproduction number (R_0)

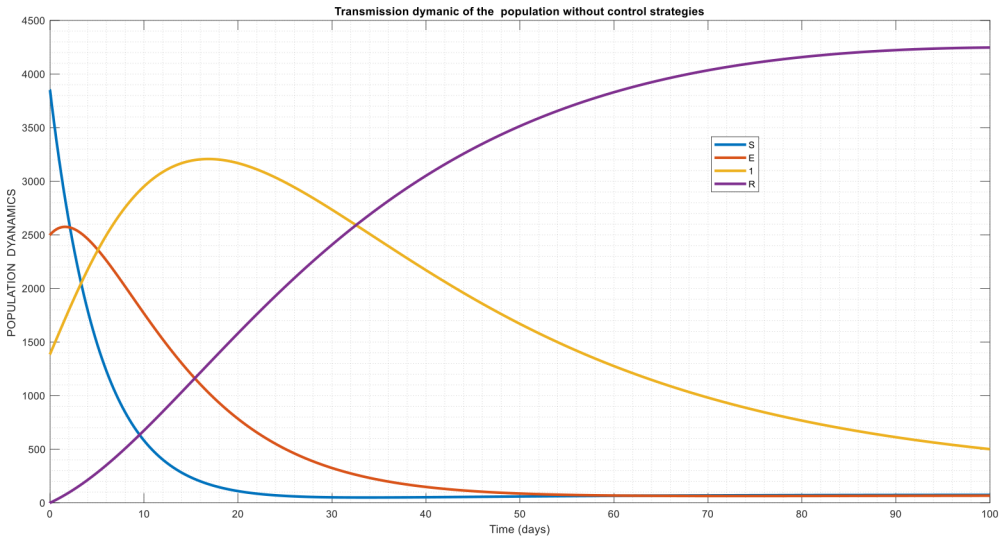

Figure 3: The trajectory solutions of the transmission of the dynamics of diphtheria

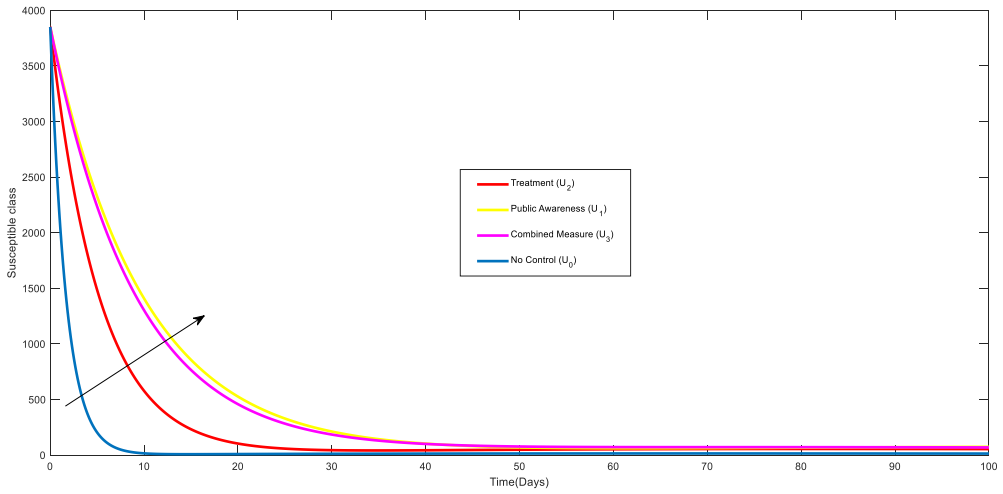

Figure 4: Solution Trajectories of the human susceptible class with control Strategies

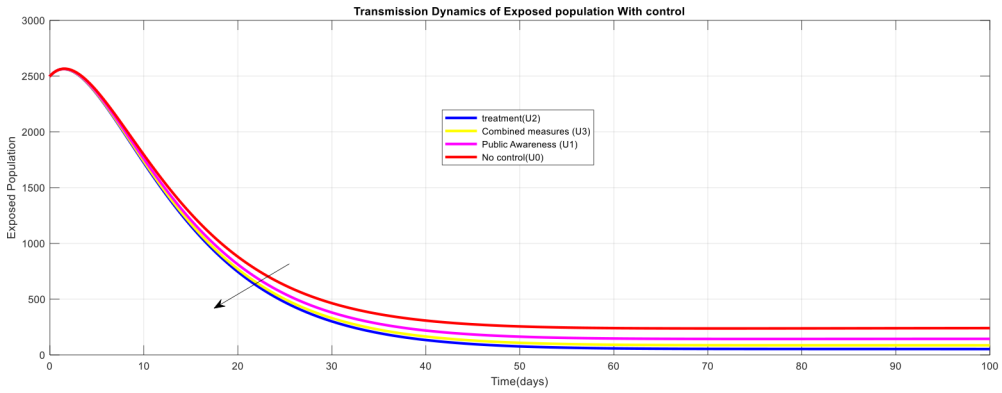

Figure 5: Trajectories solution of the exposed class with control strategies

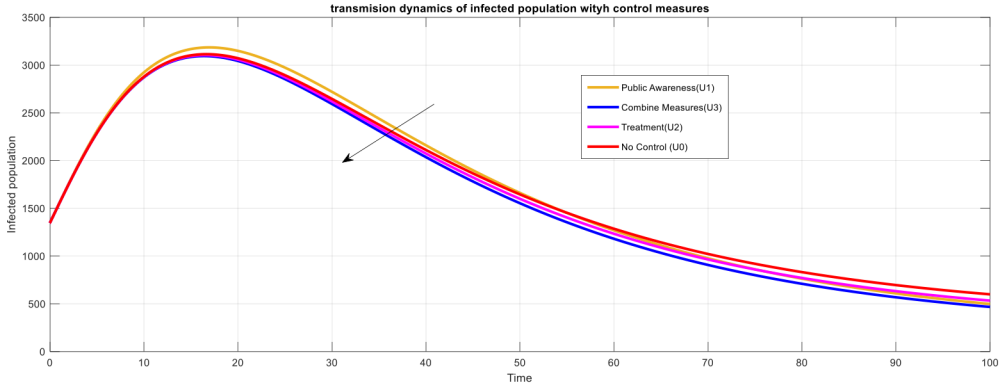

Figure 6: Solution Trajectories of the infected population with control Strategies

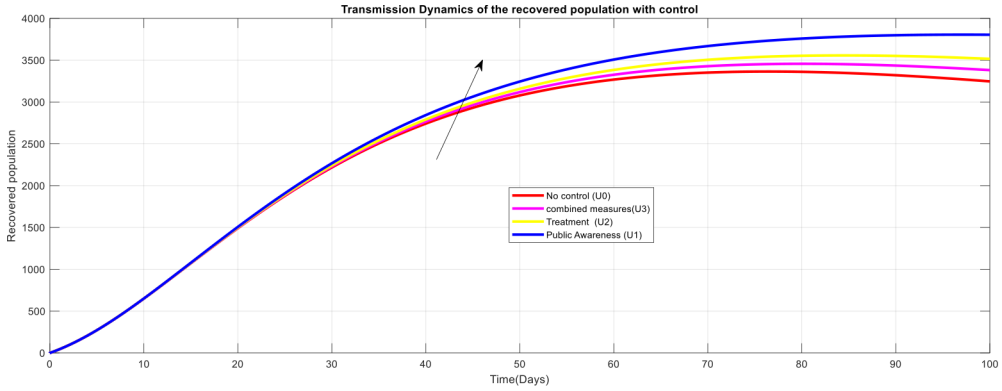

Figure 7: Solution Trajectories of the recovered population with optimal control strategies

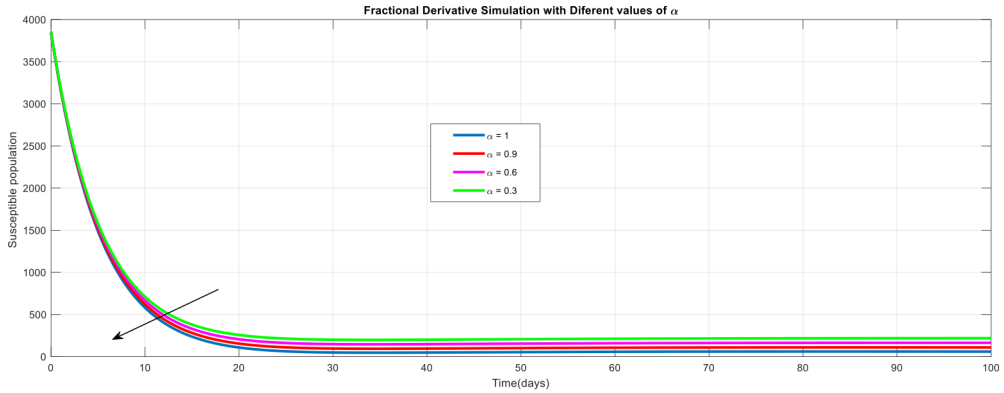

Figure 8: Solution trajectories of fractional derivation simulation with different values of α in the susceptible class

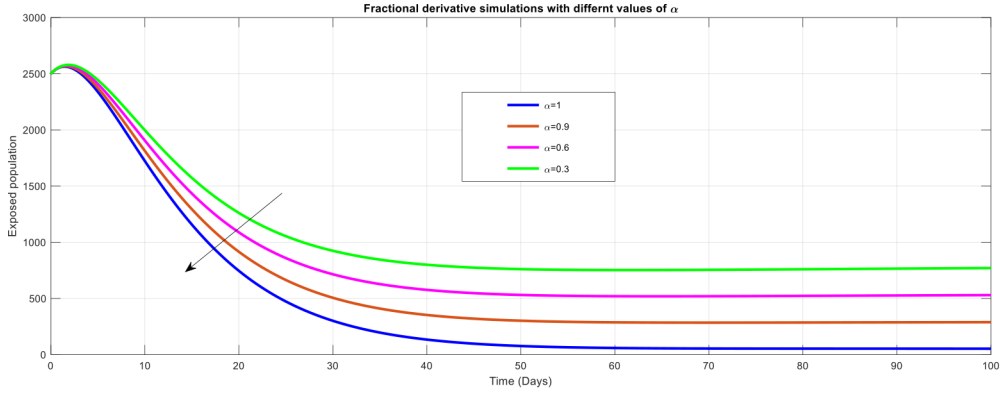

Figure 9: Solution trajectories of fractional derivation simulation with different values of α in the exposed class

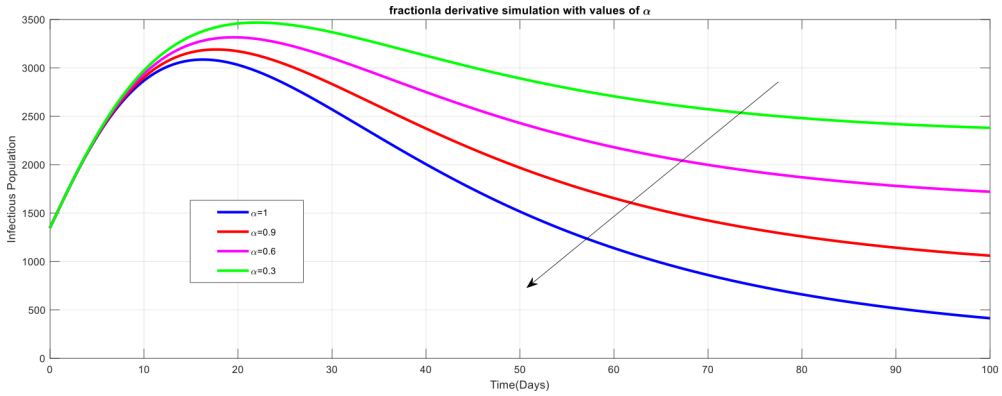

Figure 10: Solution trajectories of fractional derivation simulation with different values of α on the infected class

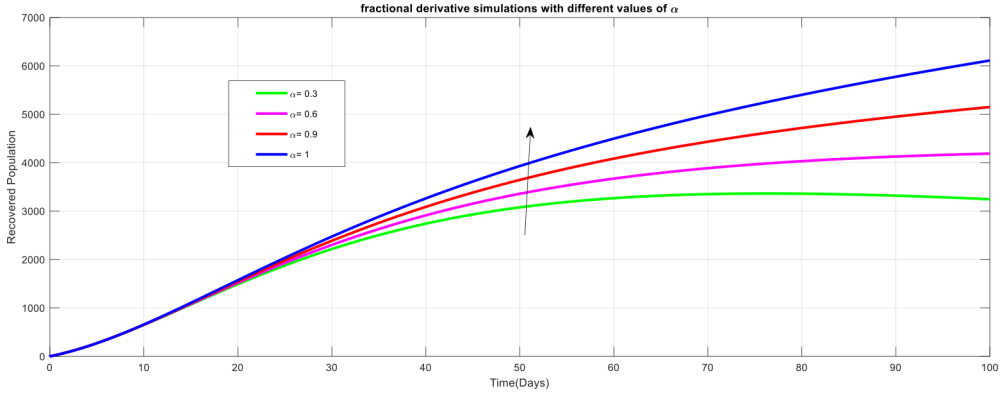

Figure 11: Solution trajectories of fractional derivation simulation with different values of α on the recovered class

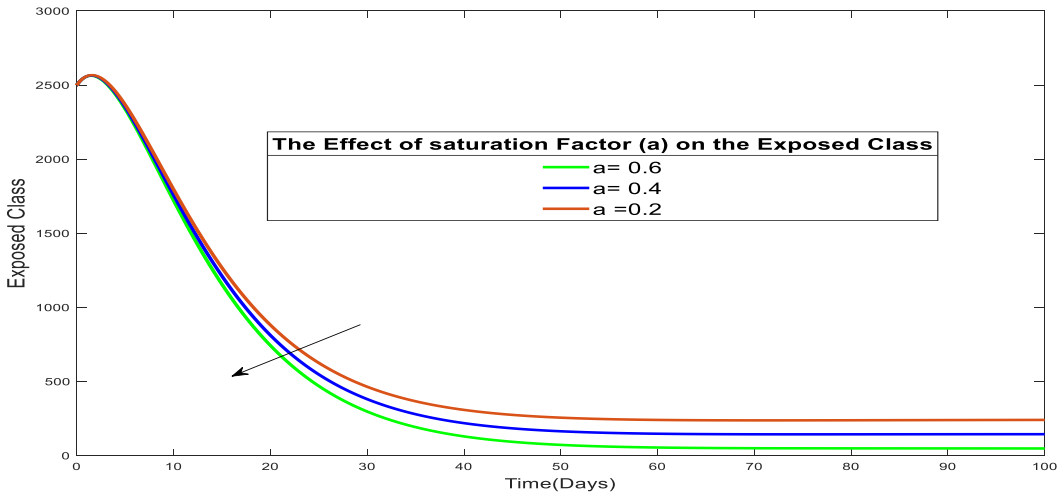

Figure 12: dynamical behavior of the saturation factor (a) on the exposed class

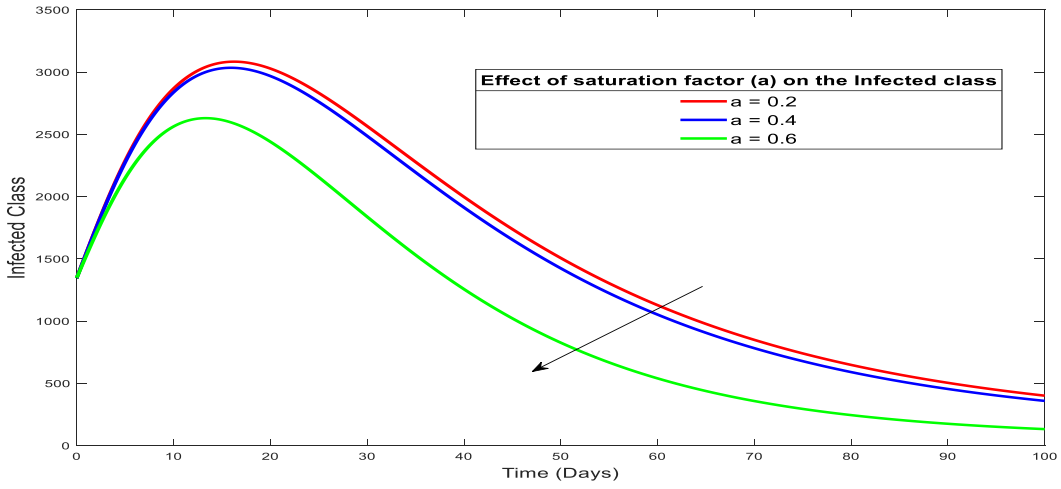

Figure 13: dynamical behavior of the saturation factor (a) on the infected class

4 Acknowledgement

We want to appreciate Mrs Adetoun Loyinmi and Aminat Ijaola for their moral support.

References

[1] Agbomola, J., Loyinmi, A. A. (2022). Mathematical model for the dynamical behavior of Ebola Transmission in human-bat population: implication of immediate discharge of recovered individuals.

[2] Agbomola, J.O, A. C. Loyinmi, (2021). Modelling the impact of some control strategies on the transmission dynamics of Ebola virus in human-bat population: An optimal control analysis. Heliyon, 8(12).

[3] Amalia P.S, Toaha, Kasbawati, (2022) Optimal control of mathematical model of diphtheria spreading, Daya Matematis: Jurnal Inovasi Pendidikan Matematika 10 (2) 2022, 138–147.

[4] Anderson, A. What to know about diphtheria, (2022), WebMD LLC ©2005- 2025. https://webmd.com/a-to-z-guides/what-to-know-diphtheria-causes. (Accessed on 25th March 2024).

[5] Asamoah, J.K.K, Okyere E, A. Abidemi, S.E. Moore, G. Sun, Z. Jim, E. Acheampong, J.F. Gordon, (2019) Optimal control and comprehensive cost effectiveness for covid-19, Results Physics.

[6] Britannica,B. R The Editors of Encyclopaedia. ‘‘diphtheria’’, Encyclopedia Britannica, (2023), Retrieved on 6th September, 2023 from https://www.britannica.com/ science/diphtheria. (Accessed 24 february 2024).

[7] CDC, Diphtheria, 2022, https://www.cdc.gov/diphtheria/about/causestransmission.html. (Accessed on 25th March 2024).

[8] Diethelm, K. Freed A.D, (1999). The FracPECE, subroutine for the numerical solution of differential equations of fractional order. Forschung und wissenschaftliches Rechnen 57–71

[9] Diethelm K, (1997). An algorithm for the numerical solution of differential equations of fractional order. Electron. Trans. Numer. Anal. 5(1), 1–6

[10] Duru E.C. Anyanwu M.C (2023). Mathematical model for the transmission of mumps and its optimal control, Biom. Lett. 60 (1), 77–95.

[11] Geruas H. Hugo H.K, (2021). Modelling africa trypanosomiasis in human with optimal control and cost effectiveness, J. Appl. Math. Inform. 39, 895–918.

[12] Idowu, K. O. Loyinmi A. C, (2023). Impact of contaminated surfaces on the transmission dynamics of corona virus disease (Covid-19). Biomed J. Sci. Tech. Res., 51 42280-90.

[13] Idowu, K.O. Loyinmi A. C, (2023). Qualitative analysis of the transmission dynamics and optimal control of covid-19. EDUCATUM Journal of Science, Mathematics and Technology. 10(1).

[14] Ilahi„ F. Widiana (2018). A The effectiveness of vaccine in the outbreak of diphtheria: Mathematical model and simulation, IOP Conf. Ser: Mater. Sci. Eng.434 012006.

[15] Islam.M.D.Z, (2018). Developing a mathematical model for Optimal cost effectiveness treatment strategies applied to a Diphtheria outbreak (M.Sc thesis), Department of Mathematics, Bangladesh University of Engineering and Technology, Dhaka-1000, 98 pages.

[16] Kanchanarat S. Chinviriyasit, W. Chinviriyasit, (2022). Mathematical assessment of the impact of the imperfect vaccination on diphtheria transmission dynamics, Symmetry, 14 .

[17] Lamichhane A. Radhakrishnan S,(2023). Diphtheria, StatPearls [Internet], StatPearls Publishing, Treasure Island (FL), Jan-. https://www. ncbi.nlm.nih.gov/books/NBK560911/.

[18] Li C. (2009). Tao, On the fractional Adams method. Comput. Math. Appl. 58(8) 1573–1588.

[19] Loyinmi, A. C. Lateef, I. A. (2024). Fractional order model of dynamical behavior and qualitative analysis of Anthrax with infected vector and saturation. Preprints. 2024030632.

[20] Loyinmi A. C. Ajala A.S. Alani, L.I (2024) Analysis of the effect of vaccination, efficient surveillance and treatment on the transmission dynamics of cholera. Al-Bahir journal for Engineering and Pure Sciences, 5(2), 94–107.

[21] Loyinmi, AC. Gbodogbe S. O. Idowu K. O, (2023). On the interaction of the human immune system with foreign body: mathematical modeling approach. Kathmandu University Journal of Science, Engineering and Technology, 17(2) 1-17.

[22] Loyinmi, A.C. Gbodogbe S. O, (2024). Mathematical modeling and control strategies for Nipah virus transmission incorporating Bat–to–pig–to– human pathway. EDUCATUM Journal of Science, Mathematics and Technology, 11(1) 54-80.

[23] Madubueze, C.E. Gweryina, R.I. Tijani, K.A. (2021) A dynamic of typhoid fever model with optimal control analysis, J. Ratio Math. 41 2021, 255–282.

[24] NHS, Diphtheria, 2022,https://www.nhs.uk/conditions/diphtheria/. (Accessed on 25th March 2024)

[25] Oli, M.K. Venkataraman, M P.A. Klein, L.D. Wendland. Brown, (2006). Population dynamics of infectious disease: A discrete time model, Ecol. Model.198,183–194.

[26] Pang, L. Liu, S. Zhang, S. Tian, T. (2019). The cost-effectiveness and optimal strategy of the tobacco control, Comput. Math. Methods Med. . 8189270.

[27] Sweileh, W.M. (2022). Global research activity on mathematical modeling of transmission and control of 23 selected infectious disease outbreak, Glob. Health 18 (4) 2022.

[28] WHO, Diphtheria, (2017), https://www.who.int/news-room/questions-andanswers/items/diphtheria, (Accessed on 27th March 2024).

[29] Masti1, I. Sayevand K, Jafari, H. (2024) On epidemiological transition model of the Ebola virus in fractional sense. Journal of Applied Analysis and Computation, 14(3), 2024, 1625-1647.

[30] Sayevand, K. Pichaghchi. K, (2016). A fresh view on the interaction of growth rates and diffusion coefficients of cancer tumor models. Journal of Advanced Mathematical Modeling, 5(2) 2016, 1-23.